catalysts

MDPI

Article

Oxidation of Glycerol in Base-Free Aqueous Solution Using Carbon-Supported Pt and PtSn Catalyst

María L. Faroppa [1], María E. Chiosso [1,2], Juan J. Musci [1,2], Marco A. Ocsachoque [3], Andrea B. Merlo [3] and Mónica L. Casella [1,3,*]

[1] Departamento de Ciencias Básicas y Experimentales, Universidad Nacional del Noroeste de la Provincia de Buenos Aires, Roque Sáenz Peña 456, Junín 6000, Argentina; mlfaroppa@phargen.com.ar (M.L.F.); eugeniachiosso17@gmail.com (M.E.C.); jota12_88@hotmail.com (J.J.M.)
[2] Centro de Investigaciones y Transferencia del Noroeste de la Provincia de Buenos Aires (CITNOBA)—UNNOBA-UNSAdA-CONICET, Monteagudo 2772, Pergamino 2700, Argentina
[3] Centro de Investigación y Desarrollo en Ciencias Aplicadas "Dr. Jorge J. Ronco" (CINDECA)—CCT-CONICET La Plata, Universidad Nacional de La Plata, Calle 47 No. 257, La Plata 1900, Argentina; ocmarco@quimica.unlp.edu.ar (M.A.O.); andreamerlo@quimica.unlp.edu.ar (A.B.M.)
* Correspondence: casella@quimica.unlp.edu.ar; Tel.: +54-221-4211353

Abstract: In the present work, we studied the catalytic performance (activity and selectivity) of Pt supported on carbon systems and Pt modified with tin in the glycerol oxidation with H_2O_2 as the oxidising agent at atmospheric pressure, 60 °C, and base-free conditions. The glycerol conversion obtained with monometallic Pt catalyst was 37% and remained unchanged with the addition of Sn in a ratio Sn/Pt = 0.4. The two bimetallic PtSn catalysts were able to oxidise commercial glycerol to dihydroxyacetone (DHA), and the selectivity to DHA reached 97% for the bimetallic catalyst with better conversion. In the reaction with crude glycerol, the conversion obtained was around 40% for the three catalysts, and the major product observed was glyceric acid. Both dihydroxyacetone and glyceric acid are high added value products with potential applications in different areas such as organic chemistry, medical and cosmetics industries.

Keywords: glycerol; oxidation; hydrogen peroxide; PtSn/C; SOMC/M

Citation: Faroppa, M.L.; Chiosso, M.E.; Musci, J.J.; Ocsachoque, M.A.; Merlo, A.B.; Casella, M.L. Oxidation of Glycerol in Base-Free Aqueous Solution Using Carbon-Supported Pt and PtSn Catalyst. *Catalysts* **2023**, *13*, 1071. https://doi.org/10.3390/catal13071071

Academic Editor: Mário Manuel Quialheiro Simões

Received: 11 April 2023
Revised: 14 June 2023
Accepted: 23 June 2023
Published: 4 July 2023

1. Introduction

Glycerol, a by-product of biodiesel production, has been identified as a key platform molecule to produce high-added-value compounds [1]. The conversion of glycerol through different chemical reactions such as oxidation, esterification, etherification, hydrogenolysis, dehydration, etc., has been extensively investigated during the last decade [2–5]. However, only a few applications have reached industrialisation mainly due to the cost of purified glycerol. To achieve viability, many processes would have to be adapted to the use of crude glycerol, which is currently the main source of glycerol on the market. As crude glycerol purification is an expensive multi-step process, the possibility of direct conversion of glycerine could be very attractive for the industry [6]. In this work, we focused on the valorization of glycerol by oxidation.

The liquid phase glycerol (Gly) oxidation can be quite complex due to the great number of products that can be obtained, such as glyceraldehyde (GlyHD), glyceric acid (GlyA), tartronic acid (TA), glycolic acid (GlycA), dihydroxyacetone (DHA), formic acid (FA), etc. (Scheme 1), which are interesting for potential applications in the polymer and fine chemical industries. GlyHD is an industrially important compound, which can be used in organic chemistry, and in the pharmaceutical and cosmetics industries. GlyA and its derivatives have many biological functions, for example, D-glycerate, which can promote ethanol catabolism in the human body, and oligomers derived from GlyA ester,

which have trypsin activity. GlyA can also be used as a food additive. Regarding TA, it is a potentially valuable chelating agent that can be used as an intermediate for the synthesis of novel polymers, and GlycA is among the functional ingredients of antiaging formulations [2,7,8]. On the other hand, DHA is a product widely used in the cosmetics industry for artificial tans and for the treatment of vitiligo. Due to the high reactivity of DHA, it also finds an important application as a versatile raw material to obtain lactic and hydroxy pyruvic acids, and 1,2-propanediol [9]. Currently, DHA is produced through microbial fermentation of glycerol, which has low productivity and a long fermentation time. The selective oxidation of glycerol to DHA using heterogeneous catalysis is a very attractive alternative for industrial applications [8].

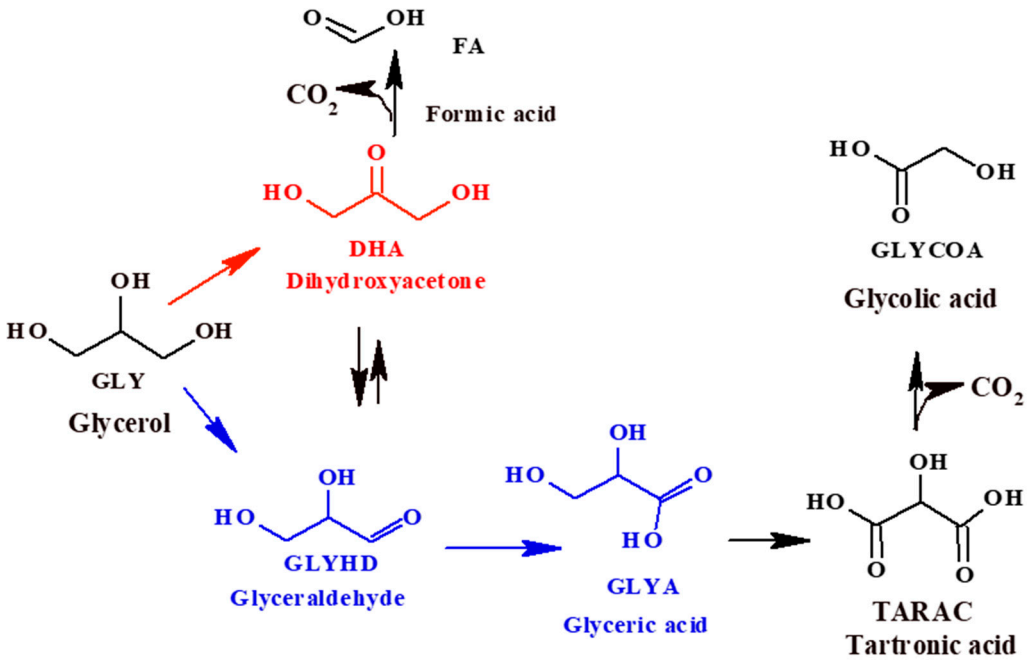

Scheme 1. Reaction products of the selective oxidation of glycerol.

The conversion and selectivity of oxidation depend on the reaction conditions (pH, temperature, catalyst-substrate ratio) and the catalyst structure (metal, particle size, and support) used [10].

Some studies recommend the use of a base for the oxidation of glycerol because the OH^- could extract a proton from the hydroxyl groups of glycerol and initiate the oxidation reaction. However, the problem with using bases is that organic salts are formed during the process, and more separation and processing steps (neutralization and acidification) are required. Over the last decades, research efforts have focused on the development of noble metal catalysts that are efficient for the oxidation of glycerol under base-free conditions [8,11–14]. Therefore, it is very attractive to explore high-efficiency catalysts for the selective oxidation of glycerol using clean oxidants such as O_2 or H_2O_2.

Heterogeneous noble metal catalysts based on Pt, Pd, and Au supported on several materials, such as carbon materials, inorganic oxides, and zeolites, together with green oxidants such as oxygen, are considered the most suitable system for the oxidation of glycerol [15–21]. For example, monometallic Pt systems without a base (Pt particles with sizes from 1.0 to 3.0 nm) were reported to be able to catalyze the oxidation of glycerol to GlyA. In particular, for Pt catalysts supported on carbon, it has been observed that they are easily deactivated during oxidation with molecular oxygen. The interaction between the carbon support and the metal particles is weak, and particle agglomeration, metal leaching, and/or strong adsorption of acids or ketones would induce the deactivation of metal catalysts [22]. To improve these results, different studies have been carried out,

including alloying Pt with other metals such as Au, Cu, Bi, Sb, and Co, which have proven to be valuable [8 and references cited therein].

It has been observed that for Pt, Pt-Cu, and Pt-Co catalysts, glycerol oxidation occurs mainly through the glycerol to GlyHD and then the GlyA pathway in a base-free solution, and GlyA is the predominant product [13,23,24]. Instead, DHA is the main intermediate of glycerol oxidation carried out with Pt-Bi and Pt-Sb catalysts [25]. The addition of Bi to supported Pt leads to enhanced catalytic activity and selectivity for the oxidation of the secondary hydroxyl group, controlling the orientation of adsorbed glycerol towards the formation of DHA. On the other hand, the addition of Sb can also improve the formation of DHA [8 and references cited therein].

In the present work, we propose studying the catalytic performance (activity and selectivity) of systems based on Pt supported on carbon and tin-modified Pt, in the oxidation of glycerol in the liquid phase. The reactions were performed with commercial glycerol (Gly) and crude glycerol (GlyC, from biodiesel production), using H_2O_2 as the oxidising agent. The bimetallic systems were obtained using techniques derived from Surface Organometallic Chemistry on Metals (SOMC/M) to study the promoting effect of Sn on the distribution of the obtained products.

2. Results and Discussion

2.1. Preparation and Characterisation of Support and Catalysts

The surface study of the carbon support by N_2 physisorption indicated that this support had a surface area of 1000 m^2 g^{-1}, calculated by the BET method, and a pore volume of 0.53 m^3 g^{-1}. These characteristics made it a suitable catalytic support for the metallic phase dispersion [26].

The Pt content of the catalysts was determined by AAS. As reported in Table 1, the results obtained were very similar to the nominal value.

Table 1. Characterisation of Pt/C and PtSny/C catalysts.

Catalyst	% Pt	Sn/Pt [1]	d_{TEM} (nm)	% D [2]
Pt/C	1.05	---	4.0	27
PtSn0.4/C	1.05	0.42	4.4	25
PtSn0.8/C	1.05	0.83	3.7	29

[1] Atomic ratio. [2] Dispersion of Pt.

PtSny catalysts were obtained by applying techniques derived from SOMC/M. This technique allows controlling the different preparation steps of the catalytic systems, giving rise to reproducible solids from the point of view of both structure and performance. The procedure consisted of the reaction between a transition metal, Pt in this case, and an organometallic compound, $SnBu_4$, in an H_2 atmosphere. Different operating conditions (temperature, nature of the support, physical state of the organometallic compound, and the monometallic precursor) were considered, as the catalytic phase obtained depends on them. The reaction was carried out in two steps. The first stage of the reaction took place between 90 and 150 °C and resulted in a system with organotin fragments anchored on the metal surface. The second step occurred between 150 and 400 °C and corresponded to the formation of a bimetallic phase in which all the organic fragments had been detached from the surface. The following equations represent these processes:

$$Pt/C + ySnBu_4 + \frac{xy}{2}H_2 \rightarrow Pt(SnBu_{4-x})_y/C + xyBuH$$

$$Pt(SnBu_{4-x})_y/C + \frac{(4-x)y}{2}H_2 \rightarrow PtSn_y/C + (4-x)yBuH$$

Extensive investigations performed by our research group have demonstrated the specificity of the reactions that take place during the preparation of bimetallic catalysts

using SOMC/M techniques. Our results revealed that all the tin added was selectively deposited on supported platinum [27,28].

Before activation, the reducibility of the catalysts was studied using temperature-programmed reduction (TPR) experiments to obtain the optimum activation temperature. TPR profiles of all the catalysts obtained, as well as that of the carbon support, are shown in Figure 1. The monometallic catalyst, Pt/C, mainly showed a reduction signal between 250 and 450 °C, with a maximum of around 400 °C, which could be assigned to the reduction of oxidised Pt species. For the bimetallic PtSn0.4/C catalyst, the maximum H_2 consumption peak is shifted to a slightly lower temperature (350 °C), however, for PtSn0.8/C the reduction peak remained around 400 °C. The hydrogen consumption in the temperature range between 250 and 450 °C could also be attributed to the reduction of Sn^{+4}/Sn^{+2} in bimetallic systems. Considering that the reduction of the tin oxides occurred at temperatures above 630 °C, this signal would indicate a strong interaction between platinum and tin. Finally, H_2 consumption from 600 °C onwards also could be associated with methane formation through the reduction of the carbon support.

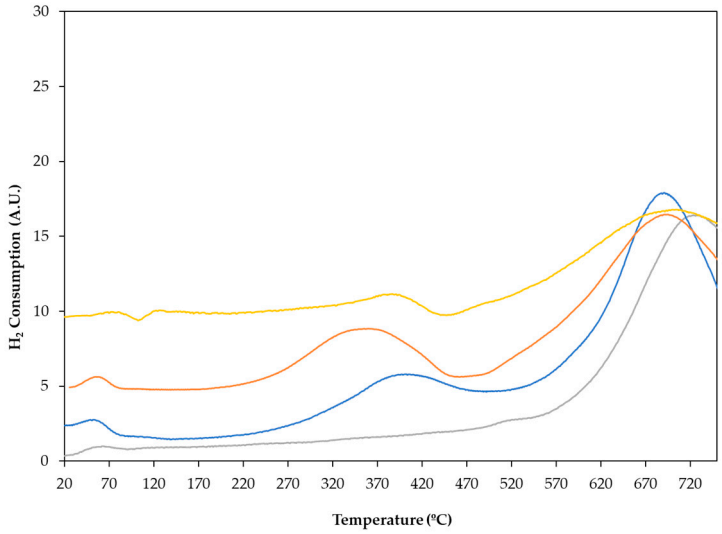

Figure 1. Temperature-programmed reduction profile for —— C support, —— Pt/C, —— PtSn0.4/C, and —— PtSn0.8/C catalysts.

Therefore, from the analysis of these profiles, the conditions for the reduction of the catalysts, 400 °C for 2 h, were obtained.

The results of the mean particle size obtained by TEM are listed in Table 1. When carrying out the preparation of bimetallic catalysts using techniques derived from SOMC/M, the addition of tin on platinum produces a slight increment in the mean particle size, which cannot be assigned to a further sintering of Pt, but to the selective deposition of tin onto it. This explains the increase in particle size from 4.0 nm on the Pt/C catalyst to 4.4 nm on the PtSn0.4/C catalyst, in agreement to what it is well established in the literature for other catalytic systems analogous to those studied here [29]. The decrease observed in the size of the metallic particles when comparing the PtSn0.8/C catalyst with the monometallic one (3.7 vs. 4.0 nm), although not very significant, could be explained by the fact that a greater amount of added tin could lead to the formation of nanoclusters with inhomogeneous size and/or composition. In Figure 2, the metal particles are well dispersed on the carbon support, with a homogeneous distribution of the active phase on the catalyst surface and no large agglomerations.

The catalysts were analysed using the XPS technique to obtain information about the oxidation states of the elements and the surface composition. Table 2 shows the binding energies (BE) for the $Pt4f_{7/2}$ and $Sn3d_{5/2}$ levels for the Pt/C, PtSn0.4/C, and PtSn0.8/C catalysts. In addition, the surface atomic ratio Sn(0)/Pt and the amount of re-

duced tin (Sn(0)/Sntotal) obtained from the integration of the corresponding XPS signals are also included.

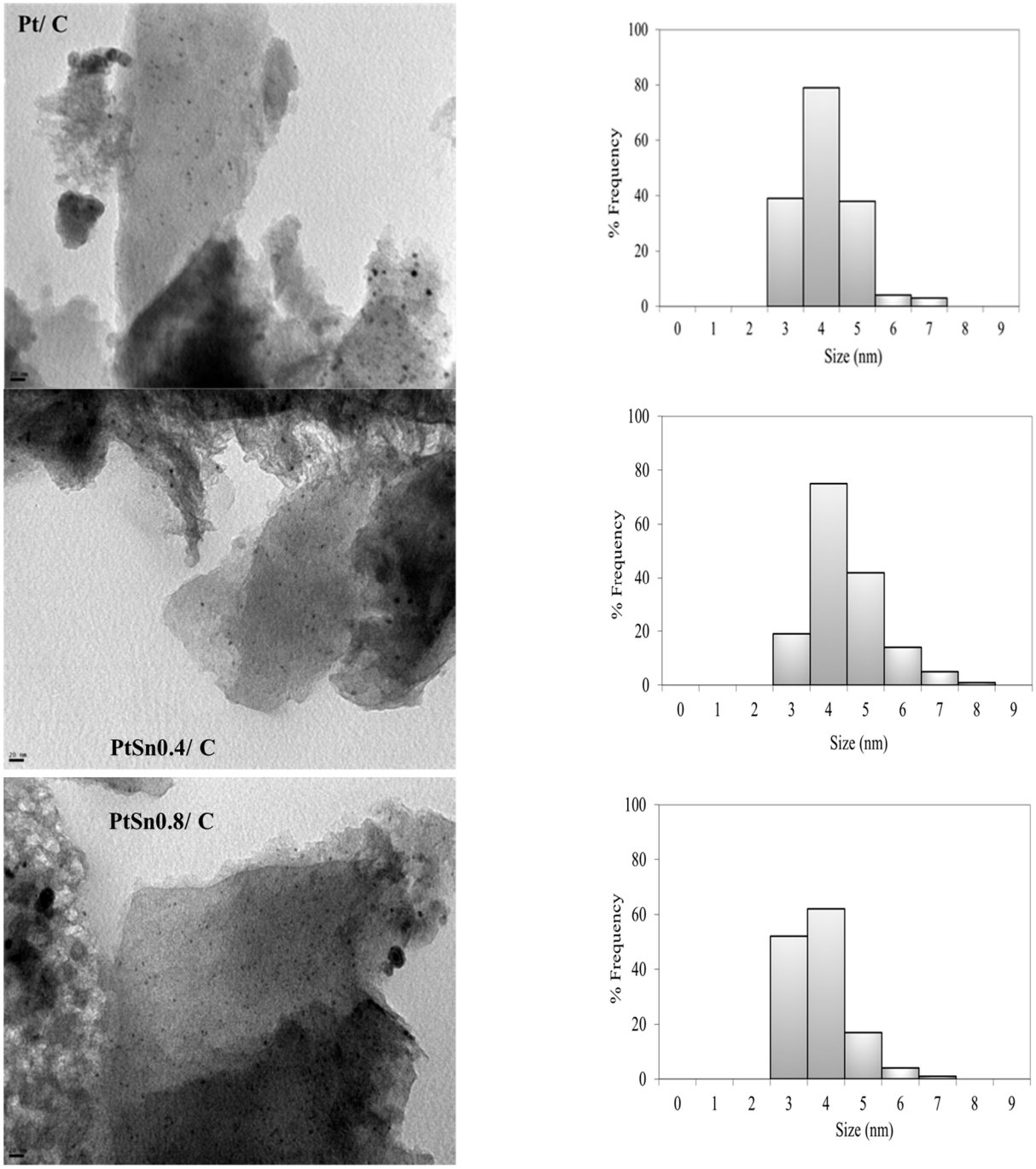

Figure 2. TEM micrographs (magnification: 270,000×) and particle size distribution of Pt/C, PtSn0.4/C and PtSn0.8/C.

The spectra of all the samples under study presented, in the Pt4f region, two signals around 71.3 and 74.9 eV corresponding to $Pt4f_{7/2}$ and $Pt4f_{5/2}$ respectively (see Supplementary Material—Figures S1–S3). The deconvolution of the $Pt4f_{7/2}$ signal showed a single peak, which is characteristic of platinum in the metallic state [30–32]. In the Pt/C sample, this peak was found at 71.3 eV, and for the bimetallic catalysts, this peak showed only a slight change in BE (0.1 eV). These results are in agreement with those reported for tin-promoted platinum catalysts prepared by SOMC/M techniques [29].

Table 2. Sn/Pt atomic ratio and binding energies (eV) of the Pt $4f_{7/2}$ and Sn $3d_{5/2}$ levels for C-supported Pt and PtSny catalysts.

Catalyst	BE Pt$4f_{7/2}$ (eV)	BE Sn$3d_{5/2}$ (eV)	Sn(0)/Sn Total [1]	Sn(0)/Pt
Pt/C	71.3	-----	------	-------
PtSn0.4/C	71.2	485.5–487.0	0.27	0.13
PtSn0.8/C	71.2	485.4–486.9	0.46	0.48

[1] Sn total = Sn(0) + Sn(II, IV).

The spectra in the Sn3d region for the PtSn0.4/C and PtSn0.8/C catalysts are shown in Figure 3. In each of them, two signals were observed around 486.9 eV and 495.4 eV, corresponding to $Sn3d_{5/2}$ and $Sn3d_{3/2}$ respectively. On the other hand, the deconvolution of the $Sn3d_{5/2}$ signal in both catalysts presented two components around 485.6 eV and 487.0 eV, which were associated with Sn(0) and Sn(II, IV) respectively [27,33–35]. It is important to note that it was not possible to distinguish between Sn(II) and Sn(IV) because their binding energies are very close [34,36]. On the other hand, the presence of metallic tin in the bimetallic catalysts could be associated with alloys generated by the preparation method. In this sense, different types of Pt-Sn alloys have been reported, such as Pt_3Sn, PtSn, Pt_2Sn_3, $PtSn_2$, and $PtSn_4$ [37]. However, the presence of such alloys is difficult to be determined by XPS analysis.

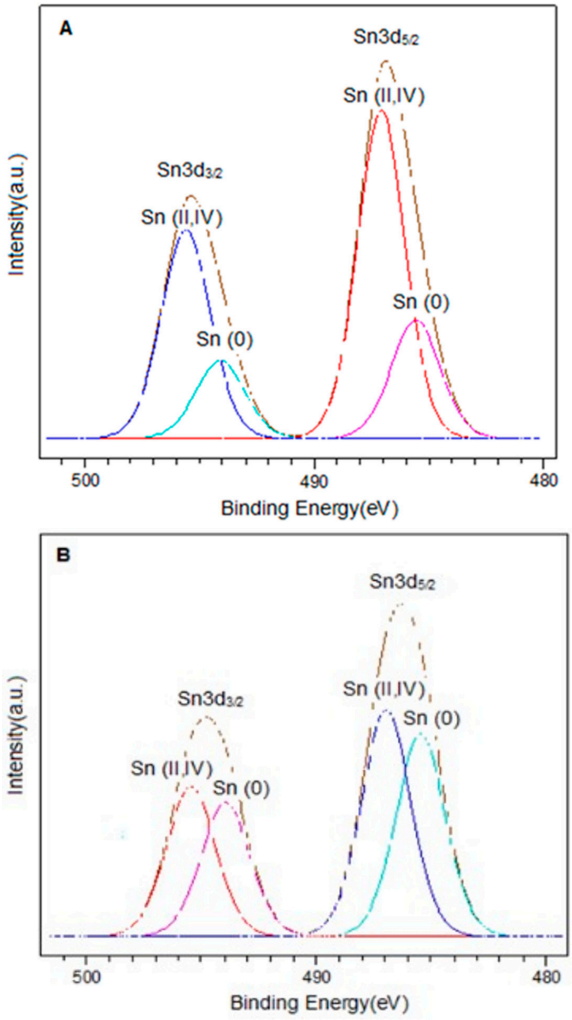

Figure 3. XPS spectra in the Sn3d region for catalysts (**A**) PtSn0.4/C and (**B**) PtSn0.8/C.

Quantitative analysis showed that for bimetallic catalysts, the Sn(0)/Sntotal ratio increased with the amount of metal. The same trend was observed for the Sn(0)/Pt ratio. This confirmed that the desired amount of tin had been deposited and was consistent with previous studies demonstrating the efficiency of the method used to obtain these catalytic systems [38,39]. From the results obtained by this technique and based on the reduction treatment applied before the oxidation reaction (2 h at 400 °C), we can assume that the bimetallic catalysts are composed of metallic Pt, metallic Sn, probably forming alloying phases with Pt, and a fraction of oxidised tin species (Sn(II)/Sn(IV)) [27,40].

2.2. Catalytic Experiments with Commercial Glycerol

First, oxidation experiments were carried out with a 0.2 mol/L aqueous solution of Gly and H_2O_2, with and without C support, in which no conversion was obtained. While it has been reported that the carbons were active per se in liquid-phase oxidation reactions [34], under the reaction conditions studied in this work, experiments showed that the reported catalytic activities were only due to the metal catalyst and not to the support.

Before the oxidation reaction, the prepared Pt and PtSny/C catalysts were reduced in hydrogen for activation, as determined from TPR profiles (2 h at 400 °C). Then, synthesised catalytic systems (100 mg) were studied in the oxidation of glycerol at 60 °C with H_2O_2 as oxidant.

Under the reaction conditions investigated, conversions of about 37% were obtained with the monometallic Pt/C and the bimetallic PtSn0.4/C catalyst, after 90 min of testing (Table 3). These results higher than those reported by other authors for the oxidation of Gly without base (NaOH) [7,10,12]. For the PtSn0.8/C system, a lower conversion (20.1%) was obtained, after 90 min of reaction. Since there was not significant difference in the particle size and dispersion of three catalysts studied, the lower turnover frequency (TOF) (see Table 3) obtained with PtSn0.8/C system, could be attributed to the tin content. Although a higher Sn addition generates a greater amount of surface SnO, which could help in the deprotonation of the hydroxyl group, the presence of this species would have interfered with the surface Pt sites that are key for the extraction of beta hydrogen. Therefore, a balance between surface Pt and SnO species would be essential for higher activity in Gly oxidation [1]. There seems to be a compromise between the dilution of Pt sites, active for the reaction, and the promoting effect of Sn, yielding the highest rates for the lower Sn/Pt ratio.

Table 3. Glycerol conversion and selectivity for the catalysts Pt and PtSny/C. Reaction conditions: 0.2 mol/L GLY, H_2O_2 as oxidant, 100 mg of catalyst, 60 °C, and 1300 rpm.

Catalysts	TOF (s^{-1})	Conversion (%) [1]	Selectivity (%) [2]				
			DHA	GlyA	TA	GlyHD	Other
Pt/C	17.6	37.0	26.0	57.1	1.7	0.3	14.9
PtSn0.4/C	20.5	36.3	96.9	1.9	1.2	--	--
PtSn0.8/C	3.0	20.1	92.3	5.2	2.1	--	0.4

[1] Reaction time: 90 min. [2] Final conversion.

On the other hand, the increase in the reaction rate when comparing PtSn0.4/C bimetallic catalysts and Pt/C, could be explained by a modification in the electronic nature of the active site [39].

Regarding the selectivity found, a large difference in the distribution of products can be observed in Table 3. For the monometallic Pt catalyst, the main product obtained was GlyA, and to a lesser extent DHA and other products. This product distribution could be explained by the predominant reaction (Scheme 1, blue way), which would start with the oxidation of the primary hydroxyl of Gly to form GlyHD (primary product) and would continue to oxidise to GlyA and to a lesser extent to DHA. Then, part of the GlyA may undergo oxidation and C-C cleavage to form GlycA and CO_2 as by-products [7]. On the other hand, for bimetallic systems, where Sn was selectively deposited on Pt sites, the

adsorption and activation of primary OH groups were not a favored pathway and therefore, DHA was preferentially obtained as an oxidation product of the secondary OH. For PtSn/C catalysts, SnO species on the surface of Pt nanoparticles could activate oxygen molecules. The oxygen atom adsorbed on the surface could function as a weak base to extract alpha protons and form a surface hydroxyl group, which could bind to H atoms on the surface to form water and be released from the catalyst surface. Simultaneously, Pt could extract beta hydrogen to produce DHA [1].

2.3. Catalytic Test—Oxidation of Crude Glycerol

Based on the results obtained with the mono- and bimetallic catalytic systems in the oxidation of commercial glycerol (Gly), tests were run with crude glycerol samples (GlyC and $GlyC_{90}$ characterised in Table 4), Pt and PtSn0.4/C systems. Oxidation tests were carried out under the same conditions as those used with Gly.

Table 4. Crude glycerol conversion and selectivity for the catalysts Pt and PtSno0.4/C. Reaction conditions: 0.2 mol/L Gly, H_2O_2 as oxidant, 100 mg of catalyst, 60 °C, and 1300 rpm.

Catalysts	Sample Gly	Conversion (%) [1]	Selectivity (%) [2]			
			DHA	GlyA	GlyHD	Other
Pt/C	GlyC	39	17.4	52.4	9.9	20.3
PtSn0.4/C	GlyC	38	14.2	79.2	5.9	0.7
PtSn0.4/C	$GlyC_{90}$	40.4	24.8	63.6	4.1	7.5

[1] Reaction time: 90 min. [2] Final conversion.

As seen in Figure 4, the plots of conversion versus time for all the studied catalysts present a certain "flattening", typical of systems that show a deactivation process. Furthermore, it is well known that platinum group metal catalysts have a marked tendency to become oxygen poisoned, either by simple blockage of adsorption sites or by over-oxidation of the metal nanoparticles. The strong adsorption of acids or ketones formed as reaction products cannot be ruled out [41]. Table 4 and Figure 4 show that there was no significant change in the conversion achieved with the monometallic catalyst and PtSn0.4/C when using the GlyC sample as a reagent. It also remained at a similar value (40.4%) to that obtained with Gly (36.3%) when oxidation performed with the treated GlyC sample and bimetallic system.

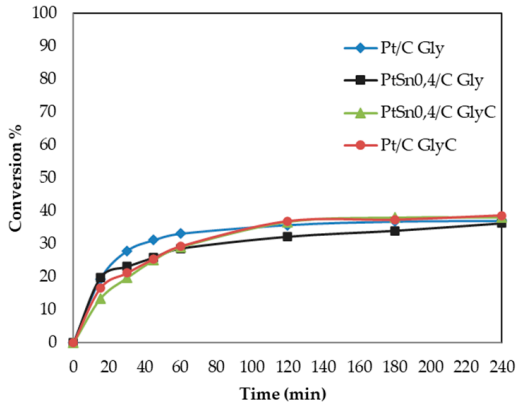

Figure 4. Oxidation of Gly (commercial) and GlyC (crude) with catalysts Pt and PtSno0.4/C. Reaction conditions: 0.2 mol/L Gly, H_2O_2 as oxidant, 100 mg of catalyst, 60 °C, and 1300 rpm.

As for the product distribution, in Tables 3 and 4 it can be observed that for the monometallic catalyst the same trend was maintained for both Gly and GlyC oxidation. In both cases, the major product was GlyA with 57.1% and 52.4% respectively. Whereas with the bimetallic PtSn0.4/C system, a drastic change in the products obtained was

observed. In the Gly oxidation test, the main product was DHA, with a selectivity of almost 97%, but when the reaction was performed with GlyC, the major product was GlyA (79.2%). This would indicate that the favored oxidation route is that of the primary OH of glycerol. This could be due to the presence of impurities in the reagent that would interfere with the reaction mechanism. An improvement in the percentage selectivity towards DHA was achieved when $GlyC_{90}$ oxidation was carried out, from 14.2% to 24.8% respectively. Thermal pretreatment of the reagent resulted in a higher percentage of Gly and the partial removal of certain impurities, such as water and methanol. However, this led to the concentration of organic impurities, MONGs, which would interfere with the selectivity of the catalytic sites [17]. This was also observed by Sullivan et al. [42] who attributed the change in catalytic behavior to the poisoning of the system within the reaction mixture. DRIFT spectra were recorded on PtSn0.4/C after the reaction with Gly and GlyC [17]. In Figure S4, no significant differences are observed for both catalysts (see Supplementary Material).

It is important to note that there are few studies in the literature describing the use of crude glycerol from the biodiesel industry, as most tests are performed using purified glycerol. Therefore, the activity results obtained with the bimetallic catalyst (PtSn0.4/C) are promising.

Finally, it could also be seen that Pt-based catalysts are deactivated during glycerol oxidation, which may be due to different factors such as weak interaction between the C support and Pt, metal leaching, agglomeration, and over-oxidation of the metal nanoparticles, and/or strong adsorption of acids or ketones formed as reaction products [8].

3. Materials and Methods

3.1. Preparation of Monometallic Catalysts

The catalyst with 1 wt% Pt was obtained by impregnation, using commercial activated carbon (C) (NORIT, ground and sieved to 60–100 mesh) as support. The preparation procedure consisted of weighing the calculated amount of the platinum salt, $(NH_4)_2[PtCl_4]$ (Sigma–Aldrich, 99.5% purity), dissolving it in water in a liquid/solid ratio of 5:1, and contacting it with the C. The system was left stirring for 24 h and then dried in an oven at 105 °C. Before use, the catalyst was activated by the reduction in H_2 flow at 400 °C for 2 h. This catalyst was named Pt/C.

3.2. Preparation of Bimetallic Catalysts

Bimetallic PtSn catalysts with atomic ratios Sn/Pt = 0.4 and 0.8 were prepared by controlled surface reactions, using techniques derived from Surface Organometallic Chemistry on Metals (SOMC/M) [37,43]. In this procedure, the Pt/C catalyst pre-reduced in H_2 was reacted with $Sn(C_4H_9)_4$ ($SnBu_4$) (Sigma-Aldrich) in a paraffinic solvent. The reaction was carried out at 90 or 150 °C, using n-heptane or n-decane as solvent (depending on the temperature used), and H_2 flow. After the reaction time had elapsed, the liquid phase was separated, and the solid was repeatedly washed with n-heptane under a N_2 flow. Finally, the catalysts were dried and reduced in H_2 flow at 400 °C for 2 h. The bimetallic catalysts obtained are designated PtSn0.4/C and PtSn0.8/C. Table 5 shows the bimetallic catalysts prepared and the reaction conditions used in each case. It also includes the atomic ratio between the two metals.

Table 5. Reaction conditions employed in the preparation of the bimetallic catalysts. Initial and final $SnBu_4$ concentration measured by gas chromatography and the atomic ratio between Sn and Pt.

Catalyst	T (°C) [1]	Wt. (g) [2]	Reaction Time (h)	C_i (mmol L^{-1}) [3]	C_f (mmol L^{-1}) [3]	Sn/Pt [4]
PtSn0.4/C	90	1.01	4.5	3.04	0.84	0.42
PtSn0.8/C	150	1.54	4.0	6.09	1.83	0.83

[1] Reaction temperature. [2] Mass of monometallic catalysts employed. [3] $SnBu_4$ concentration normalised to 1 g of Pt/C (C_i = initial concentration and C_f = final concentration). [4] Atomic ratio.

3.3. Support and Catalyst Characterisation

The surface properties and porosity of the carbon support were studied using N_2 adsorption/desorption isotherms at −196 °C, in Micromeritics ASAP 2020 equipment. The sample was degassed at 100 °C for 12 h. The surface area was calculated by the BET equation, and pore volumes were estimated by single-point adsorption in the relative pressure at P/P0 ≥ 0.99.

The Pt content was determined by atomic absorption spectroscopy (AAS). A Perkin Elmer AAnalyst 100 atomic absorption spectrometers, with an acetylene/air flame and a hollow cathode lamp, was used to analyse the samples.

The content of tin in the bimetallic PtSny/C catalysts was determined by chromatographic analysis is performed (CG-FID). The initial $SnBu_4$ solution (before obtaining the organobimetallic compound) and after 4 h of reaction was analyzed. The Ci and Cf (see Table 5) of $SnBu_4$ were determined using a calibration curve and then the moles of fixed tin were calculated by difference. Finally, with the moles of Pt used to prepare the catalyst (between 0.05 and 0.10 mmol), the Sn/Pt ratio was calculated. A Varian CP 3800 gas chromatograph, equipped with FID detector and a Factor Four capillary column (15 m × 0.25 mm ID, DF = 0.25), was used. The temperature of injector and detector was 200 °C, and for the column a program of heating from 120 °C to 200 °C, was set.

Temperature-Programmed Reduction (TPR) experiments were measured in laboratory-constructed equipment. The sample was placed in a quartz reactor and purged with Ar for 20 min to remove impurities and water. Then, the sample was heated from room temperature to 750 °C with a reductive mixture composed of 5 vol% H_2 in Ar at a flow rate of 10 mL/min. A Shimadzu GC-8A gas chromatograph equipped with a TCD detector was used for measuring hydrogen consumption.

Transmission electron microscopy (TEM) were obtained with a JEOL 100 CXII microscope. The samples were prepared by ultrasonic dispersion in distilled water. Frequency histograms of Pt particle sizes were estimated by measuring the diameter of at least 100 particles. The mean particle size (d_{TEM}) was calculated from the following Equation (1) [44]:

$$d_{TEM} = \frac{\sum_i nidi^3}{\sum_i nidi^2} \quad (1)$$

where n_i is the number of particles with size d_i.

Then, based on this information, the dispersion of Pt (D) was calculated with Equation (2) [44], assuming spherical particles:

$$D = k \times \frac{\sum_i nidi^2}{\sum_i nidi^3} \times 100 \quad (2)$$

k = 1.08 for Pt [45].

X-ray photoelectron spectroscopy (XPS) analysis was performed on a Specs Multitechnical instrument equipped with a dual Mg/Al X-ray source and a PHOIBOS 150 hemispherical analyser in Fixed Analyzer Transmission (FAT) mode. The spectra were obtained with a pass energy of 30 eV and an Al anode operated at 100 W. The pressure during the measurement was less than 2.10^{-8} mbar. Samples were supported on double-sided copper tape and then evacuated to ultra-high vacuum for at least 12 h before readings. The quantification of the species present in the catalysts was carried out using the deconvolution of the different signals of the elements, using the Casa XPS program. In all the cases, the signals were fitted with a combination of Gaussian-Lorentzian functions with a ratio of 30/70. The peak areas obtained in this way were used to determine the surface composition using the sensitivity factor method [46].

The surface chemistry was studied by Diffuse reflectance Infrared Fourier transform (DRIFT) analysed in a SHIMADZU IRAffinity-1S instrument. The dried samples were mixed with KBr in a 1:100 ratio and were scanned in the spectral range between 400 and 4000 cm^{-1}.

3.4. Catalytic Test

Several calculations were performed to ensure that the oxidation tests were measured without limitations for O_2 transport at the gas/liquid interface, without resistance to the transfer of the reagents at the liquid/solid interface and without limitations to mass transfer within the catalyst particles (see Supplementary Material).

The performance of the catalysts in the oxidation of commercial glycerol (Gly, Biopack, 99.5%) and crude glycerol (GlyC) supplied by Biobin S.A. (Junín) was studied. In the laboratory, part of the GlyC was heat-treated at 110 °C for 2 h to obtain a sample with a higher percentage of the reagent of interest, $GlyC_{90}$. BS5711-1979 (BS5711-1979 is the number of the British Standard Method of sampling and test for glycerol.) was used for the determination of the composition of crude glycerol samples (Table 6).

Table 6. Composition of GlyC samples.

Sample	% Gly	% Moisture	% Ash	% MeOH	% MONG [1]
GlyC	82	12.3	4.8	0.08	0.8
$GlyC_{90}$	90	2.4	5.4	0.01	1.9

[1] MONG: matter organic non-glycerol.

The oxidation of Gly (0.2 mol/L) in the liquid phase was carried out at atmospheric pressure in a 250 mL glass reactor with constant stirring (1300 rpm) and placed in a thermostatic bath that kept the temperature at 60 °C. In each test, 7.5 mL of 136 vol H_2O_2 (as an oxidising agent), 91 mL of distilled water, 100 mg of catalyst, and an initial pH adjusted to 5 were employed as operating conditions. The initial time was taken just before the addition of the catalyst in the reactor (see Scheme 2). The catalytic tests were run only once for each catalyst.

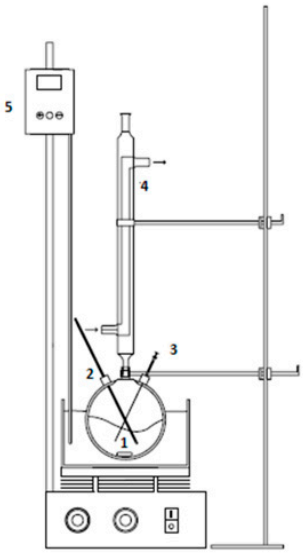

Reactor parts:

1. Magnetic diver
2. Thermometer
3. Syringe for sample collection
4. Coolant
5. Thermostat for temperature regulation with thermocouple.

Scheme 2. Scheme of the reactor used in the oxidation experiments.

To monitor the reaction, samples were taken from the reactor and analysed by liquid chromatography using UHPLC DIONEX UltiMate 3000 equipment with both a UV detector (210 nm) and a refractive index (RI) detector. The separation of the compounds was carried out in a PhenoSphere 5 µ Sax 80 A ion exclusion column at 50 °C. The eluent was 5 mmol/L H_2SO_4 (at a flow rate of 0.6 mL/min). The products were identified by comparison with commercial standards (Sigma-Aldrich).

The conversion was determined by measuring the glycerol concentration as a function of time, using Equation (3):

$$X_{Gly} = \frac{M^0_{Gly} - M^t_{Gly}}{M^0_{Gly}} \quad (3)$$

where X_{Gly} is the glycerol conversion, M^0_{Gly} is the initial molar concentration of glycerol, and M^t_{Gly} is the glycerol molar concentration at time t.

The selectivity of compound *i* (S_i) was calculated using Equation (4) [47]:

$$S_i = \frac{M^t_i}{M^0_{Gly} - M^t_{Gly}} . \frac{n_i}{3} \quad (4)$$

where M^t_i is a molar concentration of compound *i* at time *t* and n_i is the number of carbon atoms of compound *i*.

In the Supplementary Material is shown an example of the HPLC spectra used to calculate conversion and selectivity (see Figure S5).

4. Conclusions

In this study, Pt/C catalysts were prepared by impregnation method and bimetallic catalysts (PSn0.4/C and PtSn0.8/C) were obtained through SOMC/M techniques. TEM and XPS results highlighted that the desired amount of tin had been deposited and was consistent with previous studies demonstrating the efficiency of the method used to obtain these catalytic systems. All systems were evaluated in the oxidation of commercial (Gly) and crude glycerol (GlyC and $GlyC_{90}$). The results revealed that carbon-supported Pt and PtSny catalysts were active for the oxidation of glycerol under base-free conditions, but the product distribution is highly dependent on the addition of the second metal and on the purity of the Gly used. Bimetallic PtSn0.4/C catalyst showed a better behavior in terms of activity in the glycerol oxidation.

With the monometallic catalyst, similar conversions were obtained after 90 min of reaction, both for Gly and GlyC, being glyceric acid (GlyA) the main product. GlyA has many biological functions and can be used as a food additive. The addition of tin to the Pt/C catalyst produced significant changes in product distribution when Gly was used. The system with lowest Sn content (PtSn0.4/C) allowed a conversion similar to that of the monometallic system and a 97% selectivity to dihydroxyacetone (DHA). DHA is a product widely used in the cosmetics industry. However, this distribution of reaction products underwent a major change when GlyC was used; dihydroxyacetone was largely replaced by GlyA, the main product formed. Therefore, given that there are few studies in the literature describing the use of crude glycerol from the biodiesel industry, these catalysts are a promising alternative for crude glycerol transformation in value-added chemicals.

Supplementary Materials: The following supporting information can be downloaded at: https://www.mdpi.com/article/10.3390/catal13071071/s1, Figure S1. XPS spectrum of Pt4f core level for Pt/C catalyst; Figure S2. XPS spectrum of Pt4f core level for PtSn0.4/C catalyst; Figure S3. XPS spectrum of Pt4f core level for PtSn0.8/C catalyst; Table S1. Calculation of parameters at the gas/liquid interface; Table S2. Calculation of parameters at the liquid/solid interface; Table S3. Parameters inside the particle. Possible reaction mechanism; Scheme S1: Possible mechanism for oxidation of glycerol under base-free conditions over Pt and PtSn/C catalyst. Figure S4: DRIFT spectra of PtSn0.4/C after the reaction with Gly commercial and GlyC. Figure S5: HPLC chromatogram of a reaction sample with Pt0.4/C at time 0 (a) and 240 min (b). References [48–56] are cited in the supplementary materials.

Author Contributions: Conceptualization, J.J.M., A.B.M. and M.L.C.; methodology, M.L.F.; software, M.E.C. and M.A.O.; formal analysis, M.L.F., J.J.M., A.B.M. and M.L.C.; investigation, M.L.F., A.B.M. and M.L.C.; resources, M.L.C.; data curation, M.L.F.; writing—original draft preparation, M.L.F., M.E.C., J.J.M., M.A.O., A.B.M. and M.L.C.; writing—review and editing, A.B.M. and M.L.C.; supervision, J.J.M. and M.L.C.; project administration, M.L.C.; funding acquisition, M.L.C. All authors have read and agreed to the published version of the manuscript.

Funding: This research was funded by UNNOBA (project SIB 2237/2022 and project PPIC EXP 2703/2019), UNLP (project X903, EXP 100-1282/19), CONICET (project PUE 005/2018, EXP 8085/17; PIP 086/2022 and PIP 0134/2021) and ANPCyT FONCyT (PICT 2019/1962).

Data Availability Statement: Experimental research data are available upon request to the authors.

Acknowledgments: The authors would like to acknowledge the following institutions of Argentina for the financial support, UNNOBA, UNLP, CONICET and ANPCyT FONCyT (PICT 2019/1962). We thank Téc. Daiana Latorre for her collaboration in the development of catalytic experiments and HPLC analyses.

Conflicts of Interest: The authors declare no conflict of interest. The funders had no role in the design of the study; in the collection, analyses, or interpretation of data; in the writing of the manuscript; or in the decision to publish the results.

References

1. Dou, J.; Zhang, B.; Liu, H.; Hong, J.; Yin, S.; Huang, Y.; Xu, R. Carbon supported Pt_9Sn_1 nanoparticles as an efficient nanocatalyst for glycerol oxidation. *Appl. Catal. B Environ.* **2016**, *180*, 78–85. [CrossRef]
2. Zhou, C.-H.; Beltramini, J.N.; Fan, Y.-X.; Lu, G.Q. Chemoselective catalytic conversion of glycerol as a biorenewable source to valuable commodity chemicals. *Chem. Soc. Rev.* **2008**, *37*, 527–549. [CrossRef] [PubMed]
3. Anitha, M.; Kamarudin, S.K.; Kofli, N.T. The potential of glycerol as a value-added commodity. *Chem. Eng.* **2016**, *295*, 119–130. [CrossRef]
4. Chiosso, M.E.; Lick, I.D.; Casella, M.L.; Merlo, A.B. Acid functionalized carbons as catalyst for glycerol etherification with benzyl alcohol. *Braz. J. Chem. Eng.* **2020**, *37*, 129–137. [CrossRef]
5. Chiosso, M.E.; Casella, M.L.; Merlo, A.B. Synthesis and catalytic evaluation of acidic carbons in the etherification of glycerol obtained from biodiesel production. *Catal. Today* **2021**, *372*, 107–114. [CrossRef]
6. Skrzynska, E.; Zaid, S.; Girardon, J.-S.; Capron, M.; Dumeignil, F. Catalytic behavior of four different supported noble metals in the crude glycerol oxidation. *Appl. Catal. A Gen.* **2015**, *499*, 89–100. [CrossRef]
7. El Roz, A.; Fongarland, P.; Dumeignil, F.; Capron, M. Glycerol to Glyceraldehyde Oxidation Reaction Over Pt-based Catalysts Under Base-Free Conditions. *Front. Chem.* **2019**, *7*, 156. [CrossRef]
8. Yang, L.; Li, X.; Chen, P.; Hou, Z. Selective oxidation of glycerol in a base-free aqueous solution: A short review. *Chin. J. Catal.* **2019**, *40*, 1020–1034. [CrossRef]
9. Ferrari, L.; Tuler, F.; Promancio, E.; Guse, L.; García Touza, D.; Casas, C.; Comelli, R.A. Glycerol as raw material to an Argentinian biorefinery. *Catal. Today* **2022**, *394–396*, 247–255. [CrossRef]
10. Ribeiro, L.S.; Rodrigues, E.G.; Delgado, J.J.; Chen, X.; Pereira, M.F.R.; Órfaõ, J.J.M. Pd, Pt, and Pt–Cu Catalysts Supported on Carbon Nanotube (CNT) for the Selective Oxidation of Glycerol in Alkaline and Base-Free Conditions. *Ind. Eng. Chem. Res.* **2016**, *55*, 8548–8556. [CrossRef]
11. Kondrat, S.A.; Miedziak, P.J.; Douthwaite, M.; Brett, G.L.; Davies, T.E.; Morgan, D.J.; Edwards, J.K.; Knight, D.W.; Kiely, C.J.; Taylor, S.H.; et al. Base-Free Oxidation of Glycerol Using Titania-Supported Trimetallic Au–Pd–Pt Nanoparticles. *ChemSusChem* **2014**, *7*, 1326–1334. [CrossRef] [PubMed]
12. Yang, L.; He, T.; Lai, C.; Chen, P.; Hou, Z. Selective oxidation of glycerol with oxygen in base-free solution over N-doped-carbon-supported $Sb@PtSb_2$ hybrid. *Chin. J. Catal.* **2020**, *41*, 494–502. [CrossRef]
13. Liang, D.; Gao, J.; Wang, J.H.; Chen, P.; Wei, Y.F.; Hou, Z.Y. Bimetallic Pt—Cu catalysts for glycerol oxidation with oxygen in a base-free aqueous solution. *Catal. Commun.* **2011**, *12*, 1059–1062. [CrossRef]
14. Villa, A.; Veith, G.M.; Prati, L. Selective Oxidation of Glycerol under Acidic Conditions Using Gold Catalysts. *Angew. Chem. Int. Ed.* **2010**, *49*, 4499–4502. [CrossRef] [PubMed]
15. Demirel-Gülen, S.; Lucas, M.; Claus, P. Liquid phase oxidation of glycerol over carbon supported gold catalysts. *Catal. Today* **2005**, *102–103*, 166–172. [CrossRef]
16. Namdeo, A.; Mahajani, S.M.; Suresh, A.K. Palladium catalysed oxidation of glycerol—Effect of catalyst support. *J. Mol. Catal. A Chem.* **2016**, *421*, 45–56. [CrossRef]
17. Chan-Thaw, C.E.; Campisi, S.; Wang, D.; Prati, L.; Villa, A. Selective Oxidation of Raw Glycerol Using Supported AuPd Nanoparticles. *Catalysts* **2015**, *5*, 131–144. [CrossRef]

18. Carrettin, S.; McMorn, P.; Johnston, P.; Griffin, K.; Kiely, C.J.; Hutchings, G.J. Oxidation of glycerol using supported Pt, Pd and Au catalysts. *Phys. Chem. Chem. Phys.* **2003**, *5*, 1329–1336. [CrossRef]
19. Rodrigues, E.G.; Pereira, M.F.R.; Chen, X.; Delgado, J.J.; Órfão, J.J.M. Selective Oxidation of Glycerol over Platinum-Based Catalysts Supported on Carbon Nanotubes. *Ind. Eng. Chem. Res.* **2013**, *52*, 17390–17398. [CrossRef]
20. Gil, S.; Cuenca, N.; Romero, A.; Valverde, J.L.; Sánchez-Silva, L. Optimization of the synthesis procedure of microparticles containing gold for the selective oxidation of glycerol. *Appl. Catal. A Gen.* **2014**, *472*, 11–20. [CrossRef]
21. Zhou, J.; Hu, J.; Zhang, X.; Li, J.; Jiang, K.; Liu, Y.; Zhao, G.; Wang, X.; Chu, H. Facet effect of Pt nanocrystals on catalytical properties toward glycerol oxidation reaction. *J. Catal.* **2020**, *381*, 434–442. [CrossRef]
22. Sun, Y.; Li, X.; Wang, J.; Ning, W.; Fu, J.; Lu, X.; Hou, Z. Carbon film encapsulated Pt NPs for selective oxidation of alcohols in acidic aqueous solution. *Appl. Catal. B Environ.* **2017**, *218*, 538–544. [CrossRef]
23. Liang, D.; Gao, J.; Wang, J.; Chen, P.; Hou, Z.; Zheng, X. Selective oxidation of glycerol in a base-free aqueous solution over different sized Pt catalysts. *Catal. Commun.* **2009**, *10*, 1586–1590. [CrossRef]
24. Roy, D.; Subramaniam, B.; Chaudhari, R.V. Cu-Based Catalysts Show Low Temperature Activity for Glycerol Conversion to Lactic Acid. *ACS Catal.* **2011**, *1*, 548–551. [CrossRef]
25. Nie, R.F.; Liang, D.; Shen, L.; Gao, J.; Chen, P.; Hou, Z.Y. Selective oxidation of glycerol with oxygen in base-free solution over MWCNTs supported PtSb alloy nanoparticles. *Appl. Catal. B Environ.* **2012**, *127*, 212–220. [CrossRef]
26. Rodriguez-Reinoso, F. The Role of Carbon Materials in Heterogeneous Catalysis. *Carbon* **1998**, *36*, 159–175. [CrossRef]
27. Ramallo-López, J.M.; Santori, G.F.; Giovanetti, L.; Casella, M.L.; Ferretti, O.A.; Requejo, F.G. XPS and XAFS Pt L2,3-Edge Studies of Dispersed Metallic Pt and PtSn Clusters on SiO2 Obtained by Organometallic Synthesis: Structural and Electronic Characteristics. *J. Phys. Chem. B* **2003**, *107*, 11441–11451. [CrossRef]
28. Siri, G.J.; Ramallo-López, M.J.; Casella, M.L.; Fierro, J.L.G.; Requejo, F.G.; Ferretti, O.A. XPS, and EXAFS study of supported PtSn catalysts obtained by surface organometallic chemistry on metals. Application to the isobutane dehydrogenation. *Appl. Catal. A Gen.* **2005**, *278*, 239–249. [CrossRef]
29. Pastor-Pérez, L.; Merlo, A.; Buitrago-Sierra, R.; Casella, M.; Sepúlveda-Escribano, A. Bimetallic PtSn/C catalysts obtained via SOMC/M for glycerol steam reforming. *J. Colloid Interface Sci.* **2015**, *459*, 160–166. [CrossRef]
30. Ishitobi, H.; Ino, Y.; Nakagawa, N. Anode catalyst with enhanced ethanol electrooxidation activity by effective interaction between Pt-Sn-SiO_2 for a direct ethanol fuel cell. *Int. J. Hydrogen Energy* **2017**, *42*, 26897–26904. [CrossRef]
31. Wagner, C.D. *NIST X-ray Photoelectron Spectroscopy Database*; NIST: Gaithersburg, MD, USA, 1989.
32. Serrano-Ruiz, J.C.; Sepúlveda-Escribano, A.; Rodríguez-Reinoso, F. Bimetallic PtSn/C catalysts promoted by ceria: Application in the nonoxidative dehydrogenation of isobutane. *J. Catal.* **2007**, *246*, 158–165. [CrossRef]
33. Zhang, Y.W.; Xue, M.W.; Zhou, Y.M.; Zhang, H.X.; Wang, W.; Wang, Q.L.; Sheng, X.L. Propane dehydrogenation over Ce-containing ZSM-5 supported platinum–tin catalysts: Ce concentration effect and reaction performance analysis. *RSC Adv.* **2016**, *6*, 29410–29422. [CrossRef]
34. Ruiz-Martínez, J.; Coloma, F.; Sepúlveda-Escribano, A.; Anderson, J.A.; Rodríguez-Reinoso, F. Effect of tin content and reduction temperature on the catalytic behaviour of PtSn/TiO_2 catalysts in the vapour-phase hydrogenation of crotonaldehyde. *Catal. Today* **2008**, *133–135*, 35–41. [CrossRef]
35. Wagner, C.D.; Naumkin, A.V.; Kraut-Vass, A.; Allison, J.W.; Powell, C.J.; Rumble, J.R. *NIST X-ray Photoelectron Spectroscopy Database*; NIST: Gaithersburg, MD, USA, 2007.
36. Calvillo, L.; Mendez De Leoc, L.; Thompson, S.J.; Price, S.W.T.; Calvo, E.J.; Russell, A.E. In situ determination of the nanostructure effects on the activity, stability and selectivity of Pt-Sn ethanol oxidation catalysts. *Electroanal. Chem.* **2018**, *819*, 136–144. [CrossRef]
37. Massalskii, T.B. *Binary Alloy Phase Diagrams*; ASTM: Philadelphia, PA, USA, 1986.
38. Merlo, A.B.; Machado, B.F.; Vetere, V.; Faria, J.F.; Casella, M.L. PtSn/SiO_2 catalysts prepared by surface-controlled reactions for the selective hydrogenation of cinnamaldehyde. *Appl. Catal. A Gen.* **2010**, *383*, 43–49. [CrossRef]
39. Merlo, A.B.; Vetere, V.; Ruggera, J.F.; Casella, M.L. Bimetallic PtSn catalyst for the selective hydrogenation of furfural to furfuryl alcohol in liquid-phase. *Catal. Commun.* **2009**, *10*, 1665–1669. [CrossRef]
40. Pastor-Pérez, L.; Sepúlveda-Escribano, A. Low temperature glycerol steam reforming on bimetallic PtSn/C catalysts: On the effect of the Sn content. *Fuel* **2017**, *194*, 222–228. [CrossRef]
41. Besson, M.; Blackburn, A.; Gallezot, P.; Kozynchenko, O.; Pigamo, A.; Tennison, S. Oxidation with air of cyclohexanone to carboxylic diacids on carbon catalysts. *Top. Catal.* **2000**, *13*, 253–257. [CrossRef]
42. Sullivan, J.A.; Burnham, S. The selective oxidation of glycerol over model Au/TiO_2 catalysts—The influence of glycerol purity on conversion and product selectivity. *Catal. Commun.* **2015**, *56*, 72–75. [CrossRef]
43. Ferretti, O.A.; Casella, M.L.; Basset, M.; Psaro, R.; Roberto, D.; Ugo, R. (Eds.) *Modern Surface Organometallic Chemistry*; Wiley—VCH Verlag GmbH: Weinheim, Germany, 2009; pp. 239–291.
44. Musci, J.J.; Merlo, A.B.; Casella, M.L. Aqueous phase hydrogenation of furfural using carbon-supported Ru and RuSn catalysts. *Catal. Today* **2017**, *296*, 43–50. [CrossRef]
45. Bailón-García, E.; Carrasco-Marín, F.; Pérez-Cadenas, A.F.; Maldonado-Hodar, F.J. Selective hydrogenation of citral by noble metals supported on carbon xerogels: Catalytic performance and stability. *Appl. Catal. A Gen.* **2016**, *512*, 63–73. [CrossRef]
46. Wagner, C.D.; Davis, L.E.; Zeller, M.V.; Taylor, J.A.; Raymond, R.H.; Gale, L.H. Empirical atomic sensitivity factors for quantitative analysis by electron spectroscopy for chemical analysis. *Surf. Interface Anal.* **1981**, *3*, 211–225. [CrossRef]

47. Faroppa, M.L.; Musci, J.J.; Chiosso, M.E.; Caggiano, C.G.; Bideberripe, H.P.; García Fierro, J.L.; Siri, G.J.; Casella, M.L. Oxidation of glycerol with H_2O_2 on Pb-promoted Pd/γ-Al_2O_3 catalysts. *Chin. J. Catal.* **2016**, *37*, 1982–1990. [CrossRef]
48. Ramachandran, P.; Chaudhari, R. *Topics in Chemical Engineering*; Vol.2 Three phase catalytic reactors; Gordon and Breach Science: New York, NY, USA, 1983; pp. 200–251. ISBN 0677056508.
49. Gallezot, P.; Richard, D. Selective Hydrogenation of α,β-Unsaturated Aldehydes. *Catal. Rev.* **1998**, *40*, 81–126. [CrossRef]
50. Neri, G.; Bonaccorsi, L.; Mercadante, L.; Galvagno, S. Kinetic Analysis of Cinnamaldehyde Hydrogenation over Alumina-Supported Ruthenium Catalysts. *Ind. Eng. Chem. Res.* **1997**, *36*, 3554–3562. [CrossRef]
51. Meille, V.; Pestre, N.; Fongarland, P.; de Bellefon, C. Gas/Liquid Mass Transfer in Small Laboratory Batch Reactors: Comparison of Methods. *Ind. Eng. Chem. Res.* **2004**, *43*, 924–927. [CrossRef]
52. Lucas Martínez, A. Transferencia de Materia en Tanques Agitados: Disolución de Sólidos Puros. Doctoral Thesis, Facultad de Ciencias Químicas, Universidad Complutense de Madrid, Madrid, Spain, 2015. Available online: https://books.google.com.ar/books/about/Transferencia_de_materia_en_tanques_agit.html?id=caDLjgEACAAJ&redir_esc=y (accessed on 13 June 2023).
53. Cheng, N.-S. Formula for the Viscosity of a Glycerol−Water Mixture. *Ind. Eng. Chem. Res.* **2008**, *47*, 3285–3288. [CrossRef]
54. Volk, A.; Kähler, C.J. Density model for aqueous glycerol solutions. *Exp. Fluids* **2018**, *59*, 75. [CrossRef]
55. Wilke, C.R.; Chang, P. Correlation of diffusion coefficients in dilute solutions. *AIChE J.* **1955**, *1*, 264–270. [CrossRef]
56. Ma, Y.; Gan, J.; Pan, M.; Zhang, Y.; Fu, W.; Duan, X.; Chen, W.; Chen, D.; Qian, G.; Zhou, X. Reaction mechanism and kinetics for Pt/CNTs catalysed base-free oxidation of glycerol. *Chem. Eng. Sci.* **2019**, *203*, 228–236. [CrossRef]